J Biochem. 128, 11-20 (2000)

Differential Scanning Calorimetry of Light Meromyosin Fragments Having Various Lengths of Carp Fast Skeletal Muscle Isoforms[1]

Makoto Kakinuma,*,† Akimasa Hatanaka,* Hideto Fukushima,* Misako Nakaya,* Kayo Maeda,‡ Yukio Doi,§ Tatsuo Ooi,§ and Shugo Watabe*,[2]

Laboratory of Aquatic Molecular Biology and Biotechnology, Graduate School of Agricultural and Life Sciences, The University of Tokyo, Bunkyo, Tokyo 113-8657, †Department of Chemistry of Fishery Resources, Mie University, Tsu, Mie 514-8507, ‡The Institute of Physical and Chemical Research (RIKEN), Harima Institute, Kouto, Mikazuki, Hyogo 679-5148; and §Department of Food Science, Kyoto Women's University, Higashiyama, Kyoto 605-0926

Received December 2, 1999; accepted April 4, 2000

Various recombinant light meromyosin (LMM) fragments were prepared from cDNAs encoding the 10°C and 30°C types of myosin heavy chain isoforms predominantly expressed in fast skeletal muscles of the 10°C- and 30°C-acclimated carp, respectively. These included three kinds of quarter fragments, 1/4-, 2/4-, and 4/4-quarter, composed of residues 1–130, 131–270, and 401–563 from the N-terminus, respectively, as well as three halves, N-, M-, and C-half fragments, containing residues 1–301, 131–400, and 302–563, respectively, and 69K fragments of residues 1–525. Unfortunately, in spite of extensive efforts, the 3/4-quarter fragment was not expressed for both 10°C and 30°C types in our expression system using *Escherichia coli*. All the LMM fragments except for the 10- and 30-2/4 quarters for the 10°C and 30°C types, respectively, exhibited a typical pattern of α-helix in CD spectrometry. When these were subjected to differential scanning calorimetry (DSC), 30°C-type LMM fragments were all found to be more thermostable than the 10°C-type counterparts. To identify amino acid substitutions responsible for different thermostabilities between the 10°C- and 30°C-type LMMs, six mutant proteins were prepared, mainly focusing on substitutions in the C-terminal half of LMM, and subjected to DSC and CD analyses. For three mutants in which two residues of the 10°C type were replaced by those of the 30°C type, 10-S355T/T361A, 10-M415L/L417V, and 10-S535A/H536Q, the endothermic peaks in DSC increased by 1.4–2.0°C from that of the original 10°C type. The T_m values for two single-residue substitutions, 10-H449R and 10-T491I, shifted 0.8 and 1.3°C higher than that for the 10°C-type LMM, respectively, whereas the last mutant, 10-G61V, showed no change in thermostability. The finding that the difference in T_m values for major endothermic peaks from the 10-69K and 30-69K fragments was 4.6°C, which roughly corresponds to that between the original 10°C and 30°C types, suggested that the eight substitutions located in the C-terminal region of the 69K fragments (residues 302–525) are major candidates for the residues responsible for the difference in thermostability between the 10°C- and 30°C-type LMMs.

Key words: α-helix, carp, differential scanning calorimetry, light meromyosin, recombinant DNA.

Sarcomeric myosins contain an N-terminal globular head, called subfragment-1, and a C-terminal rod-like tail, which forms a coiled-coil of α-helices wound around each other from two heavy chains (*1–3*). Myosin rods having fibrous structure are easily cleaved by limited proteolysis at approximately the middle of the molecule, producing N- and C-terminal halves of subfragment-2 and light meromyosin (LMM), respectively. Fibrous proteins of the coiled-coil α-helices, such as myosin rods and tropomyosin, consist of a series of 28-amino-acid repeats, which themselves are composed of a unit of 7 amino acid residues, *a–g* (*4–8*). While hydrophobic residues predominate at positions *a* and *d*, which lie at the interface between the two α-helices (*6*), their hydrophobic interactions form the basis for the coiled-coil structure of the two α-helices. Positions *e* and *g*, where charged residues predominate, form a salt bridge between the two α-helices and further stabilize the coiled-coil structure. On the other hand, residues in the outermost positions, *b*, *c*, and *f*, are highly charged with repeating negative and positive patches spaced 14 residues apart. These charged groups are considered to mediate the packing of the myosin molecules into filaments, where the interactions between neighboring molecules are largely electrostatic (*7*, *9–12*).

[1] This study was supported in part by Grant-in-Aid for scientific research from the Ministry of Education, Science, Sports and Culture of Japan, and from the Asahi Glass Foundation

[2] To whom correspondence should be addressed Tel: +81-3-5841-7520, Fax: +81-3-5841-8166, E-mail: awatabe@mail.ecc.u-tokyo.ac.jp

Abbreviations: DSC, differential scanning calorimetry; IPTG, isopropyl-β-D-thiogalactopyranoside; LMM, light meromyosin; T_m, transition temperature; ΔC_p, molar excess heat capacity; ΔH_{cal}, calorimetric enthalpy, ΔH_{vh}, van't Hoff enthalpy, $[\theta]$, mean residue ellipticity.

It has recently been reported that carp fast skeletal muscle cells express three types of LMM isoforms in association with acclimation temperature (*13*, *14*). The carp LMM isoforms are the 10°C and 30°C types predominantly expressed in the 10°C- and 30°C-acclimated carp, respectively, together with the intermediate type, which has an intermediate structure between the 10°C and 30°C types (*14*). These isoforms, either from intact muscle or recombinant bacterial cells, exhibited clearly different thermodynamic properties as determined by differential scanning calorimetry (DSC) and CD spectroscopy (*15–17*). DSC of carp LMM isoforms expressed in *Escherichia coli* by recombinant DNAs revealed that the 10°C and 30°C types had endotherms with transition temperatures (T_m) of 35.1 and 39.5°C, respectively, at which thermal unfolding of α-helices was demonstrated by CD spectroscopy (*17*). The intermediate type exhibited two comparable endotherms with T_m values of 34.9 and 40.6°C, implying that it has intermediate thermodynamic properties, as well as intermediate primary structure, between those of the 10°C and 30°C types. In addition, a chimeric carp LMM having the 10°C and 30°C types as N- and C-terminal halves, respectively, gave the pattern of the full-length 30°C type, and the reverse combination gave that of the 10°C type (*17*). These results suggest that thermodynamic properties of the C-terminal half mostly account for thermal unfolding of the whole molecule, at least for the 10°C and 30°C types of carp LMM.

Comparison of amino acid sequences deduced from cDNA clones for the 10°C and 30°C types of carp LMM, both including 563 amino acids, showed 26 amino acid substitutions, half of which were irregularly located in the C-terminal half (*14*). Substitutions were concentrated near the C-terminal end, three residues being contained within a nonhelical C-terminal region. However, the two types exhibited no significant differences in the 28-amino-acid repeat zones or the 7-amino-acid units typical of the coiled-coil α-helices (*14*, *18*). Therefore, the differences in thermodynamic properties between the 10°C- and 30°C-type LMM isoforms appear to be determined by one or more amino acid substitutions near the C-terminal end.

In this study, various carp fast skeletal LMM fragments were prepared with recombinant DNAs and subjected to thermodynamic analyses in order to identify more precisely the region(s) implicated in thermal stability. In addition, the effects of site-directed mutagenesis on LMM thermodynamic properties were examined, focusing on 61st glycine/valine, 355th serine/threonine, 361st threonine/alanine, 415th methionine/leucine, 417th leucine/valine, 449th histidine/arginine, 491st threonine/isoleucine, 535th serine/alanine, and 536th histidine/glutamine for the 10°C- and 30°C-type LMM isoforms, respectively.

MATERIALS AND METHODS

Materials—pET-11a and pET-11d were used to construct expression vectors containing recombinant DNAs with *E. coli* strain BL21(DE3)pLysS (Novagene).

Construction of Expression Vectors for Various Carp Light Meromyosin Fragments and Point-Mutated Light Meromyosins—Expression vectors containing recombinant DNAs for various LMM fragments were constructed from expression vectors pET10 and pET30 (*17*), which encode the 10°C- and 30°C-type LMM isoforms predominantly expressed in carp fast skeletal muscles acclimated to 10 and 30°C, respectively (*14*). The N-terminal amino acid residue of the 10°C- and 30°C-type LMM isoforms corresponds to arginine-1374 of adult chicken pectoralis muscle myosin heavy chain (*19*). Recombinant DNAs encoded four quarter LMM fragments, which were composed of residues 1–130, 131–270, 271–400, and 401–563 from the N-terminus, and named 1/4-, 2/4-, 3/4-, and 4/4-quarter LMM fragments, respectively, as shown in Fig. 1. Three half LMM fragments containing residues 1–301, 131–400, and 302–563 were also prepared and defined as N-, M-, and C-half fragments, respectively (Fig. 1). In addition, the C-terminal deleted LMM composed of residues 1–525 was prepared and designated as 69K fragment (Fig. 1).

Insert DNA fragments were amplified by PCR (*20*) using pET10 and pET30 as templates. Locations and DNA nucleotide sequences of primers employed for PCR amplification are shown in Fig. 1 and Table I, respectively. Primers P-10T, P-30T, P-2/4T, P-3/4T, and P-4/4T contained *Nhe*I recognition sites, whereas primers P-1/4E, P-2/4E, P-3/4E, P-10E, P-30E, P-NE, and P-69KE had *Bam*HI sites. PCR products were digested with *Nhe*I and *Bam*HI, and subcloned into a *Nhe*I–*Bam*HI site of pET-11a. Two fragments of about 800 bp encoding 10- and 30-C half fragments were obtained from pET10 and pET30, respectively, by *Nco*I–*Bam*HI digestion, and subcloned into the *Nco*I–*Bam*HI site of the expression vector pET-11d.

Site-directed mutagenesis was carried out with GeneEditor™ *in vitro* Site-Directed Mutagenesis System (Promega) using expression vector pET10 as a template, together with primers P-GV (5′-CCTCATGATTGATGTGGAGAGGGC-3′), P-ST/TA (5′-AACACCAAGAAGAAGCTTGAGGCTGA-3′), P-ML/LV (5′-AAGAAGAACCTGGAGGTGACTGTC-3′), P-HR (5′-TCCAGGGTGCGTGAGTTGGAA-3′), P-TI (5′-AAGAACGTGATCCGCCTGCAGG-3′), and P-SA/HQ (5′-AGCTGGAGGAGGCTCAGGAGCGCGCTG-3′). Six expression vectors, pET10-G61V, pET10-S355T/T361A, pET10-M415L/L417V, pET10-H449R, pET10-T491I, and pET10-S535A/H536Q, encoded mutant LMMs where glycine-61, serine-355, threonine-361, methionine-415, leucine-417, histidine-449, threonine-491, serine-535, and histidine-536 of the 10°C-type LMM were replaced by valine, threonine, alanine, leucine, valine, arginine, isoleucine, alanine, and glutamine contained in the 30°C-type LMM, respectively.

The sequences of inserted DNA fragments in expression vectors were confirmed by DNA nucleotide sequencing.

Bacterial Expression and Protein Purification—Plasmids containing various expression vectors for carp LMM fragments were transformed into *E. coli* strain BL21(DE3)-pLysS. Subsequent induction of protein expression with isopropyl-β-D-thiogalactopyranoside (IPTG) and protein purification were performed essentially according to our previous paper (*17*).

Since the six mutant LMMs as well as the 30-C half fragment retained filament-forming ability, these were purified by the dilution-precipitation method. Other fragments were not precipitated in a low-ionic-strength buffer, then extracted proteins were first treated with ammonium sulfate at 50% saturation and centrifuged. The resultant supernatant was dialyzed against 50 mM Tris-HCl (pH 8.0) containing 0.5 mM DTT and applied to a DEAE-Toyopearl 650M column (1.4 × 26 cm, Tosoh) equilibrated with the same buffer. The adsorbed proteins were eluted with a linear gra-

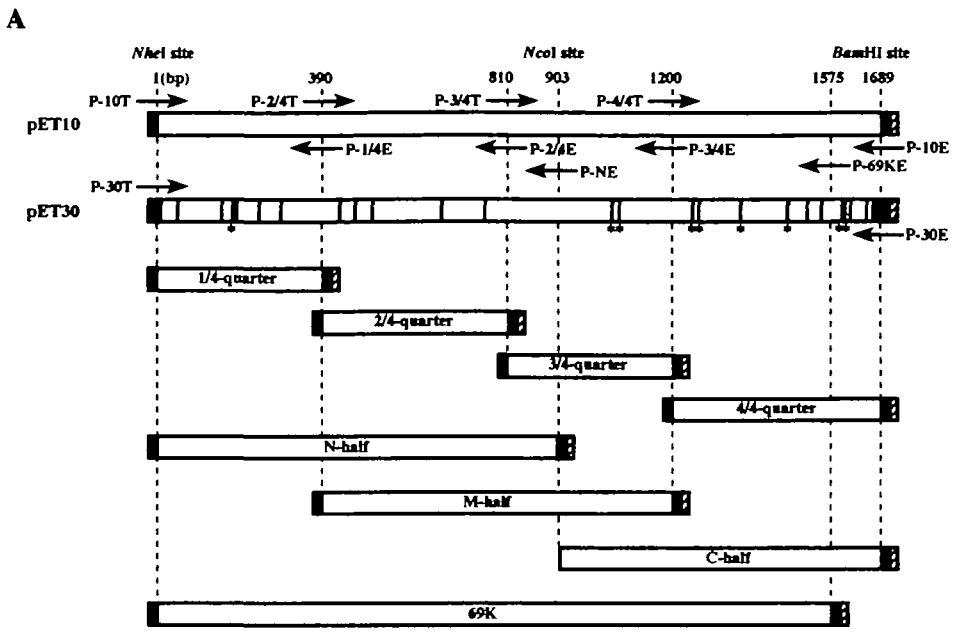

B

```
10°C-type  RAKYETDAIQRTEELEESKKKLAQRLQDAEESIEAVNSKCASLEKTKQRLQSEVEDLMIDGERANAL  67
30°C-type  .T..............A.................................G.........V....S.

10°C-type  AANLDKKQRNFDKVLADWKQKYEESQAELEAAQKEARSLSTELFKMKNSYEEALDHLETLKRENKNL 134
30°C-type  ..............E.............G.....................................

10°C-type  QQEISDLSEQLGETGKSIHEIEKAKKTVESEKAEIQTALEEAEGTLEHEESKILRVQLELNQVKSEI 201
30°C-type  .......T............L...........S.....................................

10°C-type  DRKLAEKDEEMEQIKRNSQRVLDSMQSTLDSEVRSRNDALRVKKKMEGDLNEMEVQLSHANRQAAEA 268
30°C-type  ......................I.................................I.............

10°C-type  QKQLRNVQGQLKDAQLHLDEAVRGQEDMKEQVAMVERRNSLMQAEIEELRAALEQTERGRKVAEQEL 335
30°C-type  ..........................................................!.........

10°C-type  VDASERVGLLHSQNTSLINSKKKLETDLVQVQGEVDDAVQEARNAEEKAKKAITDAAMMAEELKKEQ 402
30°C-type  ....................T.....A.....................................

10°C-type  DTSAHLERMKKNMEIIVKDLQHRLDEAESLAMKGGKKQLQKLESRVEELEAEVEAEQRRGADAVKGV 469
30°C-type  ............I.M.................................R.....................

10°C-type  RKYERRVKELTYQTEEDKKNVLRLQDLVDKLQLKVKAYKRQAEEAEEQANTHLSRYRKVQHELEESH 536
30°C-type  ......................I..............V...........T................AQ

10°C-type  ERADIAESQVNKLRAKSREAGKTKVEE                                       563
30°C-type  ....V.............D...S.D..
```

Fig. 1. **Schematic representation of the coding sequences for various carp light meromyosin fragments (A) and comparison of amino acid sequences of the 10°C- and 30°C-type light meromyosin isoforms (B).** pET10 and pET30 are expression vectors encoding carp 10°C- and 30°C-type LMM isoforms, respectively, composed of 563 amino acid residues (*17*). Vertical bars in the coding sequence for the 30°C-type LMM indicate codons for amino acid substitutions compared with the 10°C-type LMM. Arrows indicate the positions of primers. Shaded, light-shaded, and hatched rectangles represent stop codon, *Nhe*I site, and *Bam*HI site, respectively. The 1/4-, 2/4-, 3/4-, and 4/4-quarter fragments consist of residues 1–130, 131–270, 271–400, and 401–563 from the N-terminus, respectively, while the N-, M-, and C-half fragments are composed of residues 1–301, 131–400, and 302–563, respectively. The C-terminal deleted LMM, designated to 69-K fragments, contains residues 1–525. Amino acid sequences of LMMs are cited from Imai *et al* (*14*). Asterisks in the coding sequence for the 30°C-type LMM and boxes in amino acid sequences indicate codons for amino acid residues and amino acid substitutions, respectively, used for preparation of point-mutated 10°C-type LMMs.

dient from 0 to 1.0 M KCl in the same buffer. Fractions containing LMM fragments were collected, concentrated by ultrafiltration, and dialyzed against 50 mM potassium phosphate (pH 6.8) containing 0.2 M KCl, 0.5 mM DTT, and 1 mM EDTA. LMM fractions thus obtained were further purified by high-speed gel filtration with a TSK G3000SWG column (2.15 × 60 cm, Tosoh) equilibrated with the same buffer.

Expressed proteins were confirmed by N-terminal amino acid sequencing (*21*) with a Perkin Elmer Applied Biosystems model 476A protein sequencer after SDS-PAGE (*22*).

Protein concentrations were determined by the biuret method (*23*), using bovine serum albumin as the standard.

CD Spectroscopy and Differential Scanning Calorimetry—CD measurements were performed as reported previously (*17*) with samples dissolved in 50 mM Tris-HCl (pH 8.0) containing 0.6 M KCl, 5 mM $MgCl_2$, and 1 mM DTT with a JASCO J-700W spectropolarimeter using a 0.2 mm water-jacketed cylindrical cell. The cell temperature was controlled by circulating thermoregulated water with Uni Cool LC-55N (EYELA). α-Helical contents were calculated according to Yang *et al.* (*24*).

DSC was carried out in the same buffer used for CD spectrometry with a MicroCal model MC2 differential scan-

TABLE I. **Nucleotide sequences of primers used for PCR amplifications of DNA fragments encoding various carp light meromyosin fragments.**

Primer	Nucleotide sequence
P-10T [a]	5'-GAGGTGGCCGCTAGCAGAGCCAAATATGAGACTGATGC-3' [b]
P-30T	5'-GAGGTGGCTGCTAGCAGAACCAAATATGAGACTGATGCC-3'
P-2/4T	5'-CTCGAGACCCTAAAGGCTAGCAACAAGAATCTGCAACAGGAG-3'
P-3/4T	5'-CAGGCTGCTGAGGCCGCTAGCCAGCTCAGGAACGTCCAAGGA-3'
P-4/4T	5'-ATGGCTGAGGAGCTGGCTAGCGAGCAGGACACCAGTGCTCAC-3'
P-1/4E	5'-AATCTCCTGTTGCAGGGATCCTCACTCCCTCTTTAGGGTCTCGAG-3'
P-2/4E	5'-TTGTCCTTGGACGTTGGATCCTTATTTCTGGGCCTCAGCAGCCTG-3'
P-3/4E	5'-CAGGTGAGCACTGGTGGATCCTTACTTCTTCAGCTCCTCAGCCAT-3'
P-10E	5'-AGTTTCGGATCCTCATTCTTCAACTTTAGTCTTCCC-3'
P-30E	5'-GATGGCGGATCCTCATTCTTCATCCTTGCTCTTCCC-3'
P-NE	5'-CCTGCGGGATCCTTAGGCCACCTGCTCCTTCATGTCC-3'
P-69KE	5'-AATCGGATCCTTAGTACCTGGACAGGTGAGTGTGG-3'

[a]Refer to Fig. 1 for locations of primers. [b]Single and double underlines indicate *Nhe*I and *Bam*HI recognition sequences, respectively.

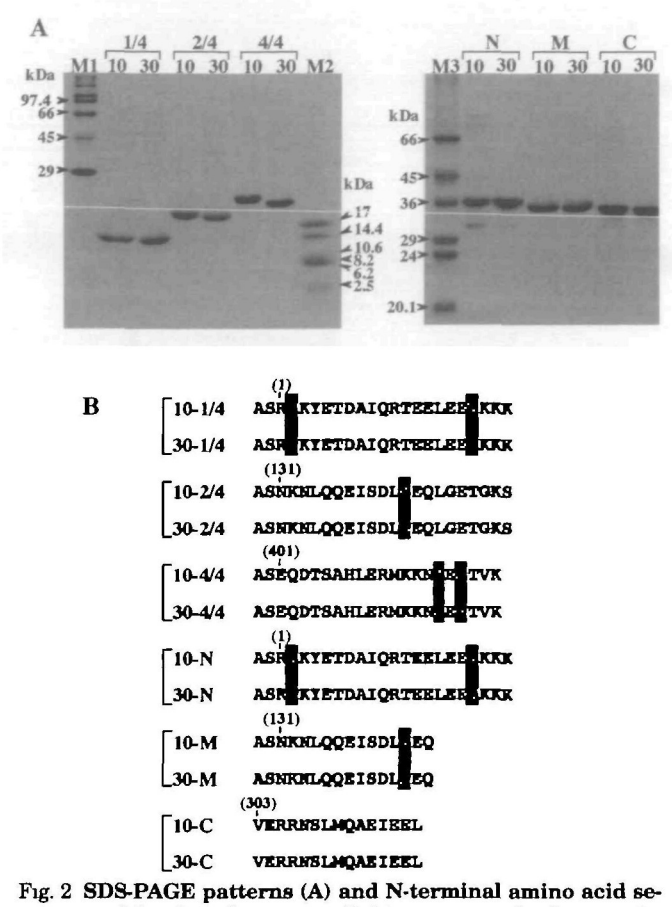

Fig. 2 **SDS-PAGE patterns (A) and N-terminal amino acid sequences (B) of various carp light meromyosin fragments.** SDS-PAGE for LMM fragments was performed with 15 and 20% gels and each lane contained approximately 5 μg of sample. Molecular weight markers (M1–3) from Sigma are composed of phosphorylase *b* (97.4 kDa), bovine serum albumin (66 kDa), ovalbumin (45 kDa), glyceraldehyde-3-phosphate dehydrogenase (36 kDa), carbonic anhydrase (29 kDa), trypsinogen (24 kDa), trypsin inhibitor (20.1 kDa), myoglobin (17 kDa), myoglobin I & II (14.4 kDa), myoglobin I & III (10.6 kDa), myoglobin I (8.2 kDa), myoglobin II (6.2 kDa), and myoglobin III (2.5 kDa). Numerals 10 and 30 in SDS-PAGE represent the lanes which contain the 10°C- and 30°C-type LMM fragments, respectively. Light-shaded boxes in N-terminal amino acid sequences indicate amino acid substitutions between the 10°C- and 30°C-type LMM fragments. Numerals in parentheses represent number of residue from the N-terminus of LMM sequence cited from Imai *et al.* (*14*). Alanine and serine at the N-terminus are caused by addition of *Nhe*I recognition site to the 5' end of the inserted fragment. Refer to Fig. 1 for abbreviations of the LMM fragments.

ning microcalorimeter essentially according to Nakaya *et al.* (*15*, *16*). DSC scans were performed at a rate of 45°C·h^{-1} in a temperature range from 4 to 60°C with samples at concentrations of 1.4–4.9 mg·ml^{-1}. Molecular weights of various LMM fragments were obtained from their amino acid sequences and used for calculation of calorimetric enthalpy (ΔH_{cal}), van't Hoff enthalpy (ΔH_{vh}), and molar excess heat capacity (ΔC_p).

The DSC analyses provide further information on the association of molecules in solution, through the ratio of ΔH_{vh} to ΔH_{cal}: that is, the former calorimetry gives a molar unfolding heat in solution and the latter corresponds to the enthalpy of a cooperative unit associated with unfolding. Since the analyses of DSC runs were performed using every single polypeptide chain as a molar unit, $\Delta H_{vh}/\Delta H_{cal}$ is equal to the number of apparent associated molecules assuming a two-state transition for the system.

RESULTS

Bacterial Expression and Purification of Various Carp Light Meromyosin Fragments—SDS-PAGE patterns and N-terminal amino acid sequences of carp fast skeletal LMM fragments are shown in Fig. 2A. Unfortunately, for both the 10°C and 30°C types, the third quarter fragments from the N-terminus were not induced with IPTG in our expression system. Other LMM fragments, however, were successfully expressed and purified to homogeneity. All the purified proteins except for the 10- and 30-C half fragments for the 10°C and 30°C types, respectively, contained two extra amino acids, alanine and serine, due to the additional nucleotide sequence for the *Nhe*I recognition site (Fig. 2B). Such extra residues at the N-terminus were previously demonstrated to have no significant effect on the helical stability and paracrystal structures for our LMM isoforms (*17*), since these residues are rather small and neutral. Molecular weights of expressed proteins corresponded roughly to those expected from amino acid sequences (Fig. 2A). N-Terminal amino acid sequences shown in Fig. 2B indicate clearly the origin of the 10°C or 30°C type LMM with respective amino acid substitutions, while the C-half fragments do not include such a substitution in this sequence range.

As described before, only the 30-C half fragment was precipitated at a low ionic strength, indicating that the solubility of LMM was changed by the fragmentation.

CD Spectrometry and Differential Scanning Calorimetry of Various Carp Light Meromyosin Fragments—As shown in Fig. 3, CD spectra of carp LMM fragments, the 1/4-quarter, 4/4-quarter, N-half, M-half, and C-half fragments, were of typical an α-helix, having minima at 222 and 208 nm at low temperature (Fig. 3). At high temperature of around 60°C, the minima at 222 nm became smaller, and the spectra did not change appreciably with further increase in temperature. The results indicate that these fragments are in a helical state at low temperature and unfold to a denatured state with increasing temperature.

Since each fragment shows an isocircular dichroic point at 203 nm in the temperature dependence of the spectrum, the unfolding occurs in the two-states manner. The thermal unfolding of the fragments was reversible as confirmed by the recovery of the α-helix after cooling down for the CD measurements and repeated runs for the DSC measurements (data not shown).

The CD spectra for the 2/4-quarter fragments from the 10°C and 30°C types were similar to those of unfolded proteins, indicating that these fragments were not helical under the present environmental conditions.

α-Helical contents calculated from the minimum at 222 nm are listed in Table II. As illustrated in Fig. 3, each 10°C-type fragment was lower in α-helical content than the 30°C-type counterpart, the extent being different from one fragment to another. Contents of 70–86% for the M and C-half fragments, which are about 270 and 260 residues long, respectively, are similar to those of full-length carp LMM (about 560 residues) expressed by recombinant DNAs (*17*). In contrast, the N-half fragment of a similar size (about 300 residues) has a smaller content of 60–65%, which are comparable to those of the shorter 1/4- and 4/4-quarter fragments, 38–61%. The content of the 30-4/4 quarter fragment was much higher than that of the 10-4/4 quarter counterpart.

The molar excess heat capacities, ΔC_p, obtained by DSC are shown in Figs. 4 and 5 together with the temperature dependence of residual ellipticities for the quarter and half fragments. The peaks in DSC runs were low for the 1/4-quarter fragments from the 10°C and 30°C types, corre-

TABLE II. **α-Helical contents of various carp light meromyosin fragments.**

LMM fragment	α-Helical content (%)	
	10°C type	30°C type
1/4-quarter	47[a] (10 3)[b]	56 (19 8)
4/4-quarter	38 (20.0)	61 (20 0)
N-half	60 (10.7)	65 (11 5)
M-half	78 (20.3)	86 (20.5)
C-half	70 (19.1)	71 (18.8)

[a]α-Helical contents were calculated from the mean residue ellipticity, $[\theta]$, at 222 nm shown in Fig 3 according to Yang *et al.* (*24*). [b]Measuring temperature (°C).

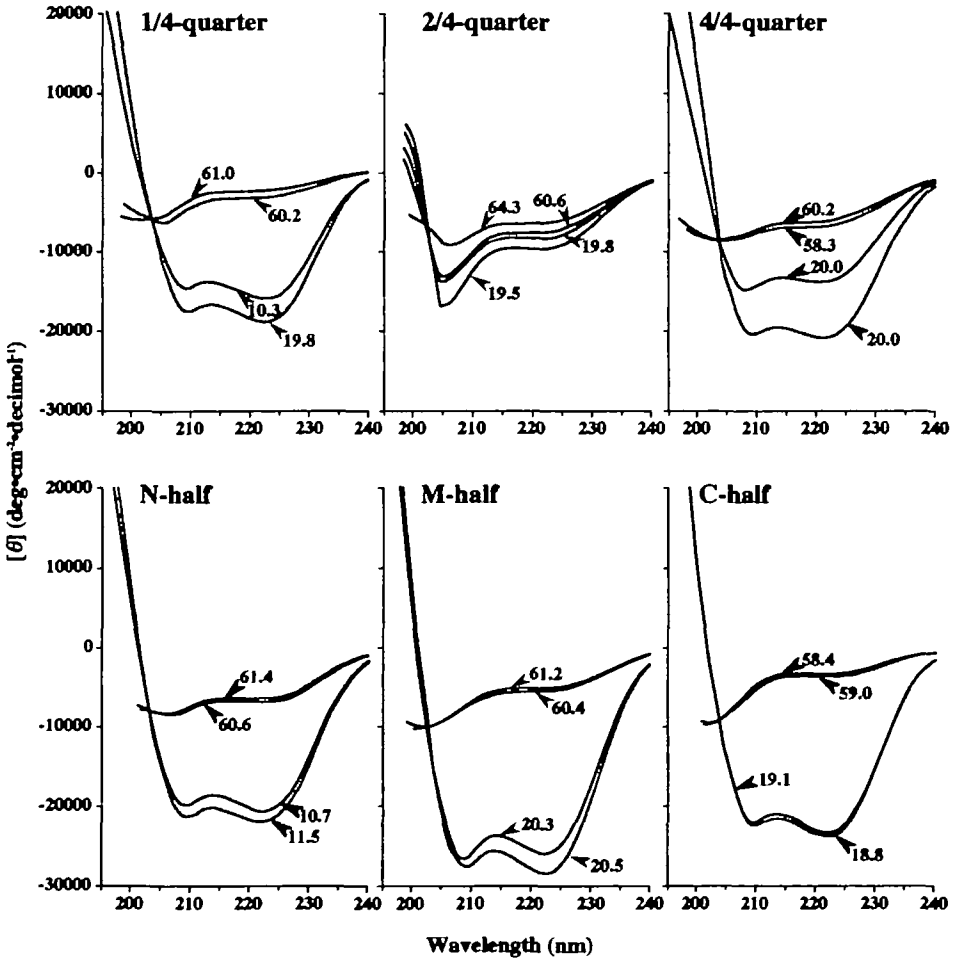

Fig. 3. **CD spectra of various carp light meromyosin fragments.** Each panel shows patterns for the 10°C- (black lines) and 30°C-type (gray lines) LMM fragments. CD spectrometry was performed in 50 mM Tris-HCl (pH 8 0) containing 0.6 M KCl, 5 mM $MgCl_2$, and 1 mM DTT. $[\theta]$ represents the mean residue ellipticity. Protein concentrations were from 1.4 and 4 0 mg·ml^{-1}, and measurement temperatures are shown in insets.

sponding to low α-helical contents of the fragments (Fig. 4). The values of T_m for both fragments were around 37°C: two peaks of 21 1°C and 36.7°C and two overlapped peaks of 29.6°C and 38.1°C for the 10- and 30-1/4 quarter fragments, respectively (Table III). These T_m values corresponded approximately to the maxima of decreasing rate derivatives of ellipticities as shown in Fig. 4, A and C. The temperature dependence of $[\theta]$ and the heights of the ΔC_p suggest that the 30-1/4 quarter is more stable than the 10-1/4 quarter fragment.

A clear difference was observed between the 10- and 30-4/4 fragments (Fig. 4, B and D). Corresponding to a greater α-helical content for the 30-4/4 quarter fragment, a large endothermic peak with T_m at 32.3°C was obtained (Table III). Plots of $[\theta]$ against temperature and their derivatives against temperature were coincident with the calorimetric results (Fig. 4D). While the 10-4/4 quarter fragment showed one major peak at 46.0°C with three minor peaks, all these peaks had very small ΔC_p values compared to that of a large peak for the 30-4/4 fragment (Fig. 4B). Thus, the 30-4/4 fragment was much more thermostable than the 10-4/4 fragment.

The results of DSC and CD analyses at different temperatures for three half-size LMMs are illustrated in Fig. 5. The M- and C-half fragments showed single major endothermic peaks with high ΔC_p values compared to the quarter LMM fragments. On the other hand, the N-half fragment exhibited two major peaks at around 20°C and 60°C (Fig. 5A): 20.8 and 61.2°C for the 10-N half fragment, and 24.2 and 58.4°C for the 30-N half fragment (Table III). Thus, the latter type had a higher T_m value for the major peak at around 20°C than the former by 3.4°C, corresponding to those obtained from the analyses of the temperature dependence of $[\theta]$ (Fig. 5D). The M- and C-half fragments from the 30°C and 10°C types exhibited single major peaks with higher T_ms for the 30- than 10-half fragments: 34.9°C compared with 32.9°C for the M-half, and 34.7°C compared with 29.2°C for the C-half fragment (Fig. 5, B and C and Table III). These endothermic peaks corresponded well to those determined by the CD analyses shown in Fig. 5, E and F.

Values of T_m and ΔH_{vh} could be also obtained from the temperature dependence of $[\theta]$ as listed in Table III, and these values were in agreement with those from DSC data, implying that the unfolding of α-helices is the major event for the present system. Since $\Delta H_{vh}/\Delta H_{cal}$ is equal to the number of apparent associated molecules, the values shown in Table III indicate that the fragments form a dimer or an oligomer as a unit of transition. That is, the LMM fragments which exhibited high α-helical contents,

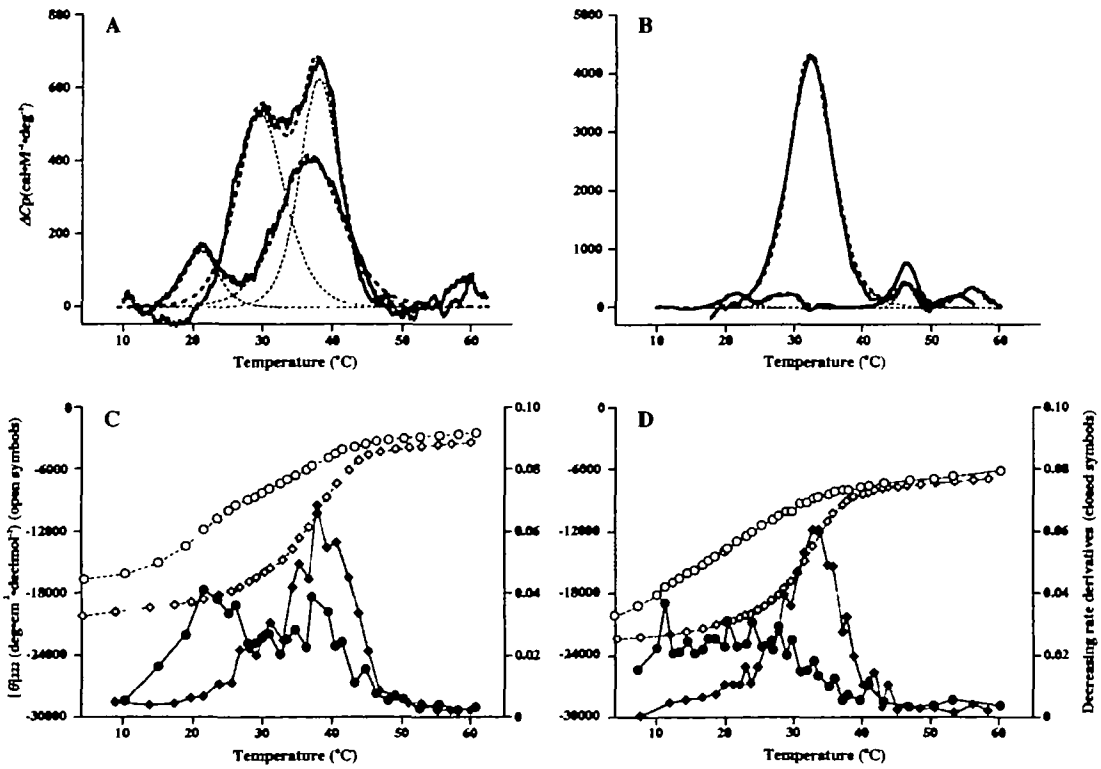

Fig. 4. **DSC scans and decreasing rate derivatives of the mean residue ellipticity against measuring temperatures for quarter light meromyosin fragments of carp.** Panels A and B show DSC patterns for the 1/4- and 4/4-quarter fragments, respectively, together with computer-calculated differential endotherms by the convolution analysis. Black and gray lines represent the 10°C- and 30°C-type LMM fragments, respectively. DSC scans were performed in 50 mM Tris-HCl (pH 8.0) containing 0.6 M KCl, 5 mM $MgCl_2$, and 1 mM EDTA, and protein concentrations were from 1 4 to 2.6 mg·ml^{-1}. The observed DSC patterns (solid lines) were subjected to smoothing treatment (bold-faced dashed lines) and convolution analysis (dotted lines) for differential endotherms. The scan rate was 45°C h^{-1}, and data were collected every 15 s. ΔC_p represents molar excess heat capacity Panels C and D show the mean residue ellipticity, $[\theta]$, at 222 nm (open symbols) and its decreasing rate derivatives ($d[\theta]/dT$) (closed symbols) of the 1/4- and 4/4-quarter fragments, respectively. The decreasing rate derivatives were calculated from the increment of $[\theta]$ at 222 nm per unit change of temperature. Circles with black lines and rectangles with gray lines represent the 10°C- and 30°C-type LMM fragments, respectively.

the N-, M-, and C-half fragments from the 10°C and 30°C types together with the 30-4/4 quarter fragment, may have formed a coiled-coil structure in solution, since their values were from 1.5 to 2.4, except for that of the 30-C half fragment, which was 4.1.

The above results indicate that all fragments except for the 10- and 30-2/4 quarter fragments form α-helical conformation; those from the 30°C type are always more thermostable than the 10°C-type fragments; and the C-terminal side fragments have higher T_m values than the N-terminal side fragments, because of the sequence differences.

CD Spectrometry and Differential Scanning Calorimetry of Carp Point-Mutated Light Meromyosins—To locate the residues responsible for the different thermostability of the 10°C- and 30°C-type carp LMMs, six mutant proteins were prepared, mainly carrying substitutions in the C-terminal half of LMM, and purified to homogeneity using the same technique as used before (*17*) (data not shown). These were 10-G61V, 10-S355T/T361A, 10-M415L/L417V, 10-H449R, 10-T491I, and 10-S535A/H536Q LMMs, where glycine-61, serine-355, threonine-361, methionine-415, leucine-417, histidine-449, threonine-491, serine-535, and histidine-536 of the 10°C-type LMM were replaced by valine, threonine, alanine, leucine, valine, arginine, isoleucine, alanine, and glutamine of the 30°C-type LMM, respectively.

The six mutant LMMs showed typical patterns of an α-helix in CD spectrometry at around 20°C, and unfolded patterns at around 60°C. Endothermic patterns for the mu-

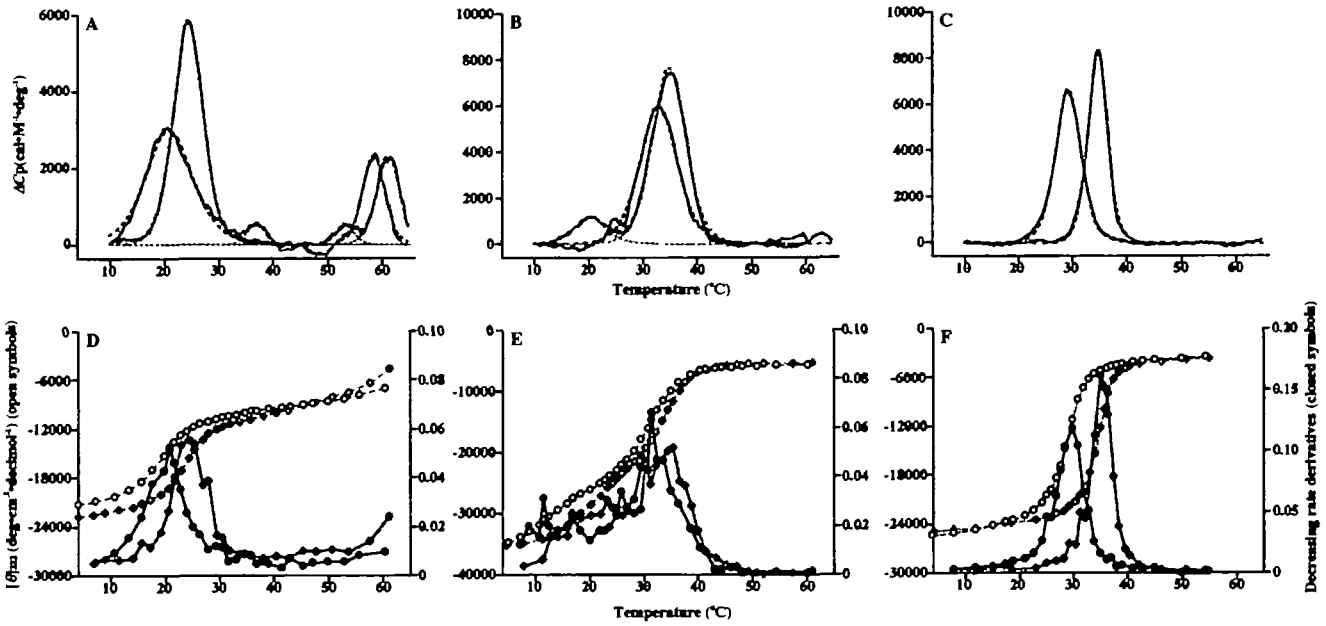

Fig. 5 **DSC scans and decreasing rate derivatives of the mean residue ellipticity against measuring temperatures for half light meromyosin fragments of carp.** Panels A, B, and C show DSC patterns for the N-, M-, and C-half fragments, respectively, together with computer-generated differential endotherms calculated by convolution analysis. Black and gray lines represent the 10°C- and 30°C-type LMM fragments, respectively. DSC scans were performed at protein concentrations from 2.4 to 4.0 mg·ml^{-1}. Panels D, E, and F show the mean residue ellipticity, [θ], at 222 nm (open symbols) and its decreasing rate derivatives (d[θ]/dT) (closed symbols) for the N-, M-, and C-half fragments, respectively. Circles with black lines and rectangles with gray lines represent the 10°C- and 30°C-type LMM fragments, respectively. Refer to the legend of Fig. 4 for other experimental conditions of DSC scans and the decreasing rate derivatives.

TABLE III **Thermodynamic parameters for thermal unfolding of various carp light meromyosin fragments.**

LMM fragment	10°C type				30°C type			
	T_m (°C)	ΔH_{cal} (kcal mol^{-1})	ΔH_{vh} (kcal mol^{-1})	$\Delta H_{vh}/\Delta H_{cal}$	T_m (°C)	ΔH_{cal} (kcal mol^{-1})	ΔH_{vh} (kcal mol^{-1})	$\Delta H_{vh}/\Delta H_{cal}$
1/4-quarter[a]	21.1	1.0	105.3	105.3	29.6	5.0	77.6	15.5
	36.7	4.9	65.3	13.3	38.1 (37.0)[b]	4.7	102.4 (57.2)	21.8
4/4-quarter[c]	21.5	1.1	156.8	142.5	32.3 (32.9)	40.0	88.2 (80.5)	2.2
	28.4	1.3	138.3	106.4	46.0	1.3	288.7	222.0
	46.0	3.0	203.8	67.9	55.4	1.9	153.2	80.6
	53.5	0.9	189.5	210.6				
N-half[d]	20.8 (19.6)	33.8	60.0 (71.5)	1.8	24.2 (23.0)	41.3	100.1 (104.5)	2.4
	53.2	2.4	182.4	76.0	36.7	2.5	174.9	70.0
	61.2	13.1	157.7	12.0	58.4	12.9	159.4	12.4
M-half[e]	32.9 (33.3)	54.3	82.9 (73.7)	1.5	20.5	9.1	88.0	9.7
					34.9 (36.5)	60.6	95.8 (83.1)	1.6
C-half[f]	29.2 (28.9)	40.8	118.0 (96.8)	2.9	34.7 (34.4)	39.4	161.2 (128.7)	4.1

[a]Values obtained from Fig. 4A. Refer to Fig. 1 for abbreviations of various LMM fragments. [b]Values in parentheses obtained from the temperature dependence of [θ] in Figs. 4 and 5. [c]Values obtained from Fig. 4B. [d]Values obtained from Fig. 5A. [e]Values obtained from Fig. 5B. [f]Values obtained from Fig. 5C.

tants contained single major peaks at around 35°C followed by some minor peaks at higher temperatures. The major peaks were found to be responsible for thermal unfolding, as demonstrated by decreasing rate derivatives of $[\theta]$ (these data are not shown).

Mutant 10-G61V LMM showed no change in the T_m value compared to the original 10°C-type LMM (Table IV), indicating that the substitution of valine for glycine has little effect on the thermostability under the present environmental condition. Since the T_m value of the main peak for the 10-H449R LMM was 35.9°C, 0.8°C higher than the original 10°C-type LMM (Table IV), the substitution of arginine for histidine had a small positive effect on the thermostability. Another single residue mutant, the 10-T491I LMM showed a higher T_m value by 1.3°C (Table IV). The 10-S535A/H536Q mutant also showed about the same change in the T_m value for the 10-T499I LMM (Table IV). The T_m value of the major endothermic peaks corresponding to thermal unfolding of α-helices was 37.1°C for the 10-S355T/T361A and 10-M415L/L417V LMMs which contained two substitutions at a close range in the N-terminal region of the C-half LMM fragment (Table IV), about 2.0°C higher than the original 10°C-type LMM (*17*). These results suggest that the accumulation of small contributions to thermostability of LMM by individual amino acid substitutions in the C-terminal region of LMM produces the difference in thermostability between the 10°C- and 30°C-type LMMs.

CD Spectrometry and Differential Scanning Calorimetry of Carp Carboxy-Terminal-Deleted Light Meromyosins—To confirm the results from the mutant proteins, C-terminal-deleted LMM, designated to 69K LMM fragment, was prepared and subjected to DSC and CD analyses. The deleted region, which is composed of 38 residues, has 6 amino acid differences (Fig. 1).

The 69K fragments from the 10°C and 30°C types exhibited two major peaks in DSC runs (Fig. 6A). Judging from the temperature dependence of $[\theta]$ (Fig. 6B), the T_m values of the major endothermic peaks corresponding to the thermal unfolding of α-helices were 34.2 and 38.8°C for the 10-69K and 30-69K fragments, respectively (Table V). The difference of 4.6°C in the T_m values for the major endothermic peaks of the 10-69K and 30-69K fragments roughly corresponded to that in the thermostabilities between the original 10°C and 30°C types, suggesting that the six substitutions contained in the 38 residues from the C-terminus of LMM had little influence on the thermodynamic properties of LMM isoforms.

TABLE IV. **Thermodynamic parameters for thermal unfolding of carp point-mutated light meromyosins.**

LMM	T_m (°C)	ΔH_{cal} (kcal mol^{-1})	ΔH_{vh} (kcal·mol^{-1})	$\Delta H_{vh}/\Delta H_{cal}$
10°C-type[a]	35.1	114.2	156.6	1.4
	53.4	20.7	116.0	5.6
10-G61V	35.0 (35.2)[b]	100.8	156.7	1.6
	45.2	5.3	251.8	47.5
	54.2	22.9	103.1	4.5
10-S355T/T361A	35 4	54.2	103.1	1.9
	37 1 (37.3)	47 6	249 8	5.2
	61.0	13.0	182 3	14.0
10-M415L/L417V	32 2	36.7	116.4	3 2
	37 1 (36.3)	125.2	175 3	1.4
10-H449R	35 9 (36.3)	137	120 7	0.9
10-T491I	32.2	36.1	102 3	2.8
	36.4 (37.1)	98.0	145.9	1.5
10-S535A/H536Q	36.5 (36.7)	118.6	147.6	1.2
	54.9	39.4	80.7	2.0
30°C-type[a]	35.4	87.3	78.6	0.9
	39.5	59.0	212.4	3.6

[a]Cited from Kakinuma *et al.* (*17*) [b]Values in parentheses obtained from the temperature dependence of $[\theta]$.

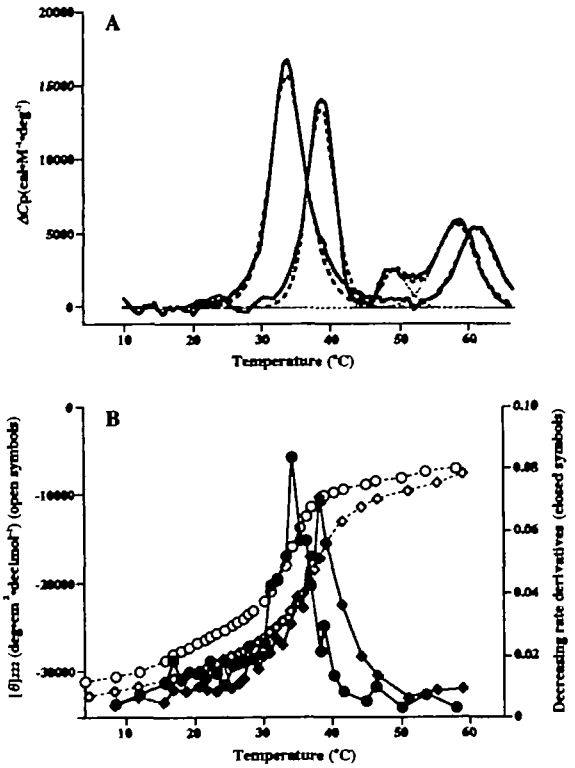

Fig 6. **DSC scans and decreasing rate derivatives of the mean residue ellipticity against measuring temperatures for carboxy-terminal-deleted light meromyosin of carp.** Panel A shows DSC patterns for the 69K fragments, together with computer-generated differential endotherms based on convolution analysis. Black and gray lines represent the 10°C- and 30°C-type LMM fragments, respectively DSC scans were performed at protein concentrations of 1 8 mg·ml^{-1} Panel B show the mean residue ellipticity, $[\theta]$, at 222 nm (open symbols) and its decreasing rate derivatives ($d[\theta]/dT$) (closed symbols) of the 69K fragments. Circles with black lines and rectangles with gray lines represent the 10°C- and 30°C-type LMM fragments, respectively. Refer to the legend of Fig. 4 for other experimental conditions of DSC scans and the decreasing rate derivatives.

TABLE V. **Thermodynamic parameters for thermal unfolding of carp 69K light meromyosin fragments.**

LMM fragment	T_m (°C)	ΔH_{cal} (kcal·mol^{-1})	ΔH_{vh} (kcal mol^{-1})	$\Delta H_{vh}/\Delta H_{cal}$
10-69K[a]	34.2 (34.1)[b]	114.6	103.9	0.9
	61.3	41.2	119 1	2.9
30-69K	38.8 (38.2)	70.0	154 6	2.2
	49.4	12.8	167.3	13.1
	58.5	46.0	112.7	2.5

[a]Values obtained from Fig. 6A. Refer to Fig. 1 for abbreviations of C-terminal deleted LMMs. [b]Values in parentheses obtained from the temperature dependence of $[\theta]$ in Fig. 6

DISCUSSION

The 10°C- and 30°C-type LMMs have the major endothermic peak responsible for thermal unfolding of α-helix at 35.1 and 39.5°C, respectively (*17*). Since the 10°C and 30°C types have only 26 amino acid substitutions in the full-length LMM molecule composed of 563 residues (*14*), certain amino acid substitutions are considered to be responsible for the differences in thermodynamic properties. Our first trial to identify such substitutions was to divide the full-length chain into four and two fragments: that is, we prepared quarter and half LMM fragments for carp 10°C- and 30°C-type LMMs by using recombinant DNAs.

Certain quarter fragments did not fold into a full α-helical conformation under the present conditions at a high ionic strength (0.6 M KCl, pH 8.0), while fragments having a longer chain length formed α-helical conformation in the same environment (Fig. 3). One of characteristic features obtained here was the difference in the 10- and 30-quarter fragments: the latter had more α-helical content than the former as illustrated in the 4/4-quarter fragments. The amino acid substitutions contained in the C-terminal side fragment appeared to contribute to their difference in the thermostability. However, the results for the quarter fragments showed that the thermostability was dependent on the chain length. For instance, the thermostability of the 10-N or 30-N half fragment consisting of the corresponding 1/4- and 2/4-quarter fragments was not additive: the unfolded 2/4-quarter fragment could form an α-helix by the connection of the chain to the 1/4-quarter fragment, since the α-helical content of the 10-N half fragment was similar to or higher than that of the 1/4-quarter fragment as seen in Fig. 3 and Table II. Thus, the results for the quarter fragments were less informative than those for the half fragments with respect to the identification of key substitutions for α-helical formation.

On the other hand, the half fragments took approximately full α-helical conformations, showing similar behaviors on CD and DSC measurements (Fig. 5 and Table III). The differences in the T_m values for the major endothermic peaks from 10°C to 30°C type were 3.4, 2.0, and 5.5°C for the N-, M-, and C-half fragments, respectively, suggesting the location of amino acid residues responsible for the thermostability, where 12, 7, and 14 substitutions are found for the above fragments, respectively.

Our second trial was the site-directed mutagenesis of the 10°C-type LMM, expecting the improvement of the thermostability by the mutation. The results showed that the replacement of glycine-61 in the 10°C type with valine had little effect on the stability, and that serine-355, threonine-361, methionine-415, luecine-417, histidine-449, threonine-491, serine-535, and histidine-536 in the 10°C type were candidates for the target residues in the difference of the T_m value (Table IV). On the other hand, the difference in T_m values for major endothermic peaks from the 10-69K and 30-69K fragments was 4.6°C, which roughly corresponded to that between the 10°C- and 30°C-type LMMs (Fig. 6 and Table V). These results suggest that the eight substitutions located in the C-terminal region of the 69K fragments (residues 302–525) are major candidates for the residues responsible for the difference in thermostability between the 10°C- and 30°C-type LMMs.

The present results suggest that the thermodynamic properties of the LMM molecules are determined not by a few crucial amino acid residues but by the accumulation of small contributions from several substitutions. Furthermore, the formation of a coiled-coil structure or an oligomer of rod-like molecules would be more favorable for the stability, and a certain minimal chain length might be requisite for the α-helical structure under the present environmental conditions.

REFERENCES

1. Lowey, S., Slayter, H.S., Weeds, A.G., and Baker, H (1969) Substructure of the myosin molecule: I Subfragments of myosin by enzymatic degradation *J Mol Biol* **42**, 1–29
2. Weeds, A.G and Pope, B (1977) Studies on the chymotryptic digestion of myosin Effects of divalent cations on proteolytic susceptibility. *J. Mol. Biol* **111**, 129–157
3. Harrington, W F. and Rodgers, M.E. (1984) Myosin. *Annu. Rev Biochem.* **53**, 35–73
4. McLachlan, A.D and Stewart, M. (1975) Tropomyosin coiled-coil interactions: evidence for an unstaggered structure. *J Mol Biol.* **98**, 293–304
5. McLachlan, A.D., Stewart, M., and Smillie, L B. (1975) Sequence repeats in α-tropomyosin *J Mol Biol* **98**, 281–291
6. Parry, D.A.D. (1981) Structure of rabbit skeletal myosin. analysis of the amino acid sequences of two fragments from the rod region *J Mol Biol.* **153**, 459–464
7. McLachlan, A.D and Karn, J. (1982) Periodic charge distributions in the myosin rod amino acid sequence match cross-bridge spacings in muscle *Nature* **299**, 226–231
8. McLachlan, A.D. and Karn, J (1983) Periodic features in the amino acid sequence of nematode myosin rod *J Mol. Biol.* **164**, 605–626
9. Atkinson, S.J and Stewart, M (1992) Molecular interactions in myosin assembly: role of the 28-residue charge repeat in the rod *J Mol. Biol.* **226**, 7–13
10. Hoppe, P.E. and Waterston, R.H (1996) Hydrophobicity variations along the surface of the coiled-coil rod may mediate striated muscle myosin assembly in *Caenorhabditis elegans. J Cell Biol.* **135**, 371–382
11. Sohn, R.L., Vikstrom, K.L., Strauss, M , Cohen, C , Szent-Györgyi, A.G., and Leinwand, L.A. (1997) A 29 residue region of the sarcomeric myosin rod is necessary for filament formation *J Mol Biol.* **266**, 317–330
12. Vikstrom, K.L., Seiler, S.H , Sohn, R L , Strauss, M., Weiss, A., Welikson, R.E., and Leinwand, L.A. (1997) The vertebrate myosin heavy chain: genetics and assembly properties. *Cell Struct. Funct* **22**, 123–129
13. Watabe, S , Imai, J., Nakaya, M., Hirayama, Y , Okamoto, Y., Masaki, H , Uozumi, T., Hirono, I., and Aoki, T. (1995) Temperature acclimation induces light meromyosin isoforms with different primary structures in carp fast skeletal muscle *Biochem. Biophys. Res. Commun.* **208**, 118–125
14. Imai, J., Hirayama, Y., Kikuchi, K., Kakinuma, M., and Watabe, S. (1997) cDNA cloning of myosin heavy chain isoforms from carp fast skeletal muscle and their gene expression associated with temperature acclimation. *J. Exp. Biol.* **200**, 27–34
15. Nakaya, M , Watabe, S., and Ooi, T. (1995) Differences in the thermal stability of acclimation temperature-associated types of carp myosin and its rod on differential scanning calorimetry *Biochemistry* **34**, 3114–3120
16. Nakaya, M., Kakinuma, M., Watabe, S., and Ooi, T. (1997) Differential scanning calorimetry and CD spectrometry of acclimation temperature-associated types of carp light meromyosin *Biochemistry* **36**, 9179–9184
17. Kakinuma, M., Nakaya, M., Hatanaka, A., Hirayama, Y., Watabe, S , Maeda, K., Ooi, T., and Suzuki, S. (1998) Thermal unfolding of three acclimation temperature-associated isoforms of carp light meromyosin expressed by recombinant DNAs. *Bio-*

chemistry **37**, 6606–6613
18. Watabe, S., Hirayama, H., Nakaya, M., Kakinuma, M., Kikuchi, K., Guo, X.-F., Kanoh, S., Chaen, S., and Ooi, T. (1998) Carp expresses fast skeletal myosin isoforms with altered motor functions and structural stabilities to compensate for changes in environmental temperature. *J. Therm. Biol.* **22**, 375–390
19. Maita, T., Yajima, E., Nagata, S., Miyanishi, T., Nakayama, S., and Matsuda, G. (1991) The primary structure of skeletal muscle myosin heavy chain: IV. Sequence of the rod, and the complete 1,983-residue sequence of the heavy chain. *J. Biochem.* **110**, 75–87
20. Saiki, R.K., Gelfand, D.H., Stoffel, S., Scharf, S.J., Higuchi, R., Horn, G.T., Mullis, K.B., and Erlich, H.A. (1988) Primer-directed enzymatic amplification of DNA with a thermostable DNA polymerase. *Science* **239**, 487–491
21. Matsudaira, P. (1987) Sequence from picomole quantities of proteins electroblotted onto polyvinylidene difluoride membranes. *J. Biol. Chem.* **262**, 10035–10038
22. Laemmli, U.K. (1970) Cleavage of structural proteins during the assembly of the head of bacteriophage T4. *Nature* **227**, 680–685
23. Gornall, A.G., Bardawill, C.J., and David, M.M. (1949) Determination of serum proteins by means of the biuret reaction. *J. Biol. Chem.* **177**, 751–765
24. Yang, J.T., Wu, C.-S.C., and Martinez, H.M. (1986) Calculation of protein conformation from circular dichroism. *Methods Enzymol.* **130**, 208–269